



Experimental investigation on criterion of three-dimensional mixed-mode fracture for concrete

Li Song*, S.M. Huang, S.C. Yang

Xi'an University of Technology, Xi'an, Shaanxi 710048, PR China

Received 9 July 2003; accepted 7 October 2003

Abstract

An investigation was carried out to establish a criterion for three-dimensional (3-D) mixed-mode fracture of concrete. Experiments on 3-D mixed-mode fracture were conducted to obtain the critical load P_{cr} . The stress intensity factor of the specimens per unit load with different combinations of K_I , K_{II} and K_{III} was calculated by the mixed hybrid finite element method. Based on the stress intensity factor per unit load and the critical load, 25 groups of critical stress intensity factors were calculated, from which a criterion for the 3-D mixed-mode fracture of concrete was derived.

© 2004 Elsevier Ltd. All rights reserved.

Keywords: Concrete; Fracture toughness; Fracture criteria

1. Introduction

The criterion of three-dimensional (3-D) mixed-mode fracture is usually preferred in the analysis of the crack propagation in huge space concrete structures, such as arch dams [1]. In the past decades, much research has been done on some fracture parameters used in the area of concrete fracture mechanics. However, most of the parameters are for the pure mode I or I–II two-dimensional (2-D) mixed-mode crack extension. With the lack of criteria for 3-D mixed-mode fracture for concrete, 3-D fracture cases often have to be simplified using 2-D fracture models in the investigation of crack problems, for instance, cracking in arch dams [2], which results in some errors.

In this paper, some experiments were designed and the test results were analyzed on the basis of the principles of linear elastic fracture mechanics. Empirical formulas for 3-D mixed-mode fracture criterion for concrete were deduced and compared to several theoretical criteria graphically.

2. Test specimen and stress intensity factor

It is well known that the 3-D critical fracture curved surface can be derived from the critical stress intensity

factors K_I , K_{II} and K_{III} . The critical stress intensity factors of specimens were obtained from the critical load P_{cr} measured at fracture in experiments, and stress intensity factors per unit load, which were calculated by the mixed hybrid finite element method [3]. The numerical calculations indicated that the ratio $K_I:K_{II}:K_{III}$ was related to the crack geometry as well as to the loading and constraint conditions applied to the specimens. To obtain the desired fracture mode, crack geometry, loading and constraint conditions of the test specimens were determined from the numerical results.

Three kinds of specimens, as shown in Fig. 1, were used to generate the different fracture modes in the experiments. The first specimen was a beam with the dimensions of $100 \times 100 \times 515$ mm. A single-edge crack was introduced to the specimen. This kind of specimen was used to form pure I, II or I–II mixed mode. The second was also a beam with the dimensions of $100 \times 100 \times 515$ mm but with a ring-shaped edge crack instead. The third was a cylindrical bar with a radius of 50 mm and a ring-shaped edge crack. This type of specimen was used to form I–III, II–III, I–II–III and pure III fracture modes.

The fracture mechanics and numerical calculations have indicated that the stress intensity factor of a 3-D crack problem usually varies with the pole angle θ [4], with the exception of pure mode III fracture for the third type of specimen with a ring-shaped edge crack. In this paper, a

* Corresponding author. Tel.: +86-029-2313100; fax: +86-029-3230026.

E-mail address: songli@xaut.edu.cn (L. Song).

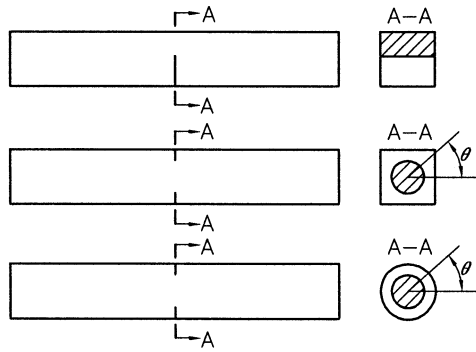


Fig. 1. Three kinds of experimental specimens.

random point at the crack front was picked at first and the stress intensity factor at that point was assumed to be the one for the entire specimen. When the K_I , K_{II} and K_{III} combination reached a critical threshold, the cracking was initiated at this point based on the principle of fracture criteria. Because the fracture criterion expression was not available until the completion of the fracture experiments, the initial position of the cracking point θ_0 was determined by the iteration method.

3. 3-D fracture experiment

3.1. Fracture experiment

Twenty-five groups of specimens with different combinations of K_I , K_{II} and K_{III} were used in the experiments. The geometry, loading and constraint conditions for each group are shown in Fig. 2. Stress intensity factors per unit load and position of cracking initiation location are listed in Table 1.

3.2. Mechanical properties and mixture proportions of concrete

The mechanical properties and mixture proportions of the concrete are listed in Table 2. The maximum grain size of the aggregate was 20 mm.

3.3. Specimen preparation

Thin steel plates with a shim at the top were fixed on the moulds and the concrete was then poured in. The mould and plates were removed after 7 days. The concrete specimens with single-edge or ring-shaped edge notches were fabricated while being cured in the moist room for 28 days.

3.4. Experimental procedures

The specimen was loaded in a universal strength tester. The critical load at fracture was recorded by an

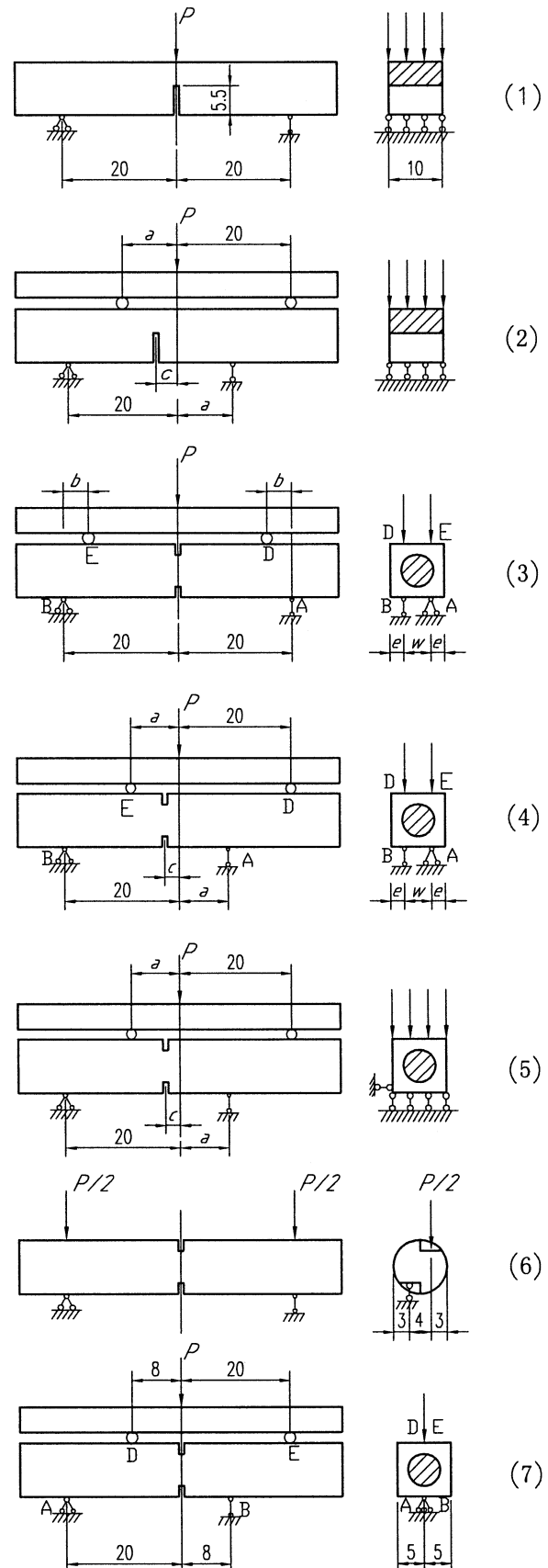


Fig. 2. The geometry, loading and constraint conditions of specimens.

Table 1
Stress intensity factor per load

Specimen No.	Figure No.	$K_I BW^{1/2}/P$	$(K_{II} BW^{1/2})/P$	$(K_{III} BW^{1/2})/P$	θ_0^a (deg)
1	Fig. 2 (1)	12.530	0.000	0.000	
2	Fig. 2 (2)	0.000	−1.192	0.000	
	$a=5, c=0$				
3	Fig. 2 (6)	0.000	0.000	2.508	
4	Fig. 2 (2)	0.404	−1.184	0.000	
	$a=5, c=0.5$				
5	Fig. 2 (2)	0.872	−1.078	0.000	
	$a=5, c=1$				
6	Fig. 2 (2)	0.812	−0.625	0.000	
	$a=10, c=2$				
7	Fig. 2 (2)	1.720	−0.664	0.000	
	$a=10, c=4$				
8	Fig. 2 (2)	2.607	−0.631	0.000	
	$a=10, c=6$				
9	Fig. 2 (3)	0.498	0.000	−1.925	−90.00
	$b=0.5, w=5$				
10	Fig. 2 (3)	0.975	0.000	−1.895	−90.00
	$b=1, w=5$				
11	Fig. 2 (3)	1.921	0.000	−1.921	−90.00
	$b=2, w=5$				
12	Fig. 2 (3)	4.660	0.000	−1.924	−90.00
	$b=5, w=5$				
13	Fig. 2 (5)	0.000	2.694	1.191	61.10
	$c=0.5, a=1$				
14	Fig. 2 (5)	0.000	0.853	0.969	39.61
	$c=0.5, a=2$				
15	Fig. 2 (5)	0.000	0.411	0.730	28.06
	$c=0.5, a=8$				
16	Fig. 2 (7)	0.000	0.276	0.841	29.69
	$c=0.5, a=8$				
17	Fig. 2 (4)	0.814	−0.343	−1.320	−139.48
	$c=0.5, a=8, w=2$				
18	Fig. 2 (4)	1.492	−0.380	−1.229	−128.54
	$c=2, a=8, w=2$				
19	Fig. 2 (5)	0.295	−0.319	−0.590	−138.91
	$c=0.5, a=8$				
20	Fig. 2 (5)	0.636	−0.303	−0.469	−130.10
	$c=1, a=8$				
21	Fig. 2 (5)	1.449	−0.293	−0.293	−113.90
	$c=2, a=8$				
22	Fig. 2 (4)	0.849	0.389	−2.583	136.41
	$c=-1, a=8, w=5$				
23	Fig. 2 (4)	0.977	0.562	−1.421	135.95
	$c=-1, a=5, w=2$				
24	Fig. 2 (5)	1.060	2.457	1.108	67.05
	$c=-0.5, a=1$				
25	Fig. 2 (5)	1.466	1.710	0.896	69.65
	$c=-1, a=1.5$				

b is the width and w is the height (or radius) of specimen. Sizes in the table are in centimeters.

* Position of initial cracking point.

electric recorder. Because of the scatter in the concrete properties, six specimens were tested in each of the 25 groups. The final critical load values P_{cr} were averaged over the maximum loads of six specimens obtained from the fracture experiments.

Table 2
The mechanical property and mixture proportion of concrete

Water (kg/m ²)	Cement (kg/m ²)	Sand (kg/m ²)	Aggregate (kg/m ²)	Compress strength (MPa)	Splitting tensile strength (MPa)
185	415	675	1104	44.2	2.86

3.5. Experimental results

The critical stress intensity factors listed in Table 3 were calculated based on P_{cr} and SIF per unit load from Table 1. A mathematical expression of 3-D mixed fracture criterion, as shown in Table 4, was derived by regressing the critical stress intensity factors from the result of the 25 specimen groups, where fracture tough-

Table 3
Critical stress intensity factor

Specimen No.	Fracture mode	P_{cr} (kN)	K_I (kN/cm ^{3/2})	K_{II} (kN/cm ^{3/2})	K_{III} (kN/cm ^{3/2})
1	I	2.35	0.93	0.00	0.00
2	II	17.30	0.00	−0.65	0.00
3	III	12.47	0.00	0.00	0.99
4	I–II	14.48	0.18	−0.54	0.00
5		12.90	0.36	−0.44	0.00
6		20.50	0.53	−0.40	0.00
7		13.18	0.72	−0.28	0.00
8		9.22	0.76	−0.18	0.00
9	I–III	13.95	0.22	0.00	−0.85
10		11.67	0.36	0.00	−0.70
11		9.54	0.58	0.00	−0.58
12		5.42	0.80	0.00	−0.33
13	II–III	6.10	0.00	0.52	0.23
14		13.70	0.00	0.37	0.42
15		23.8	0.00	0.31	0.56
16		28.57	0.00	0.25	0.76
17	I–II–III	17.47	0.45	−0.19	−0.73
18		10.80	0.51	−0.13	−0.42
19		26.77	0.25	−0.27	−0.50
20		20.87	0.42	−0.20	−0.31
21		18.32	0.84	−0.17	−0.17
22		8.93	0.24	0.11	−0.73
23		10.67	0.33	0.19	−0.48
24		6.56	0.22	0.51	0.23
25		7.76	0.36	0.42	0.22

Table 4
Mathematical expressions of mixed mode fracture criterion

Fracture model	Regressive point	Critical fracture surface equation	Related coefficient
I–II	7	$1.064K_I K_{IC} + 2.17K_{II}^2 = K_{IC}^2$	0.982
I–III	6	$1.035K_I K_{IC} + 0.923 K_{III}^2 = K_{IC}^2$	0.9945
II–III	6	$2.06K_{II}^2 + 0.927K_{III}^2 + 0.096 K_{II} K_{III} = K_{IC}^2$	0.89
I–II–III	25	$1.16K_I K_{IC}^2 + 2.096K_{II}^2 + 0.87K_{III}^2 + 0.6255 K_{II} K_{III} = K_{IC}^2$	0.91

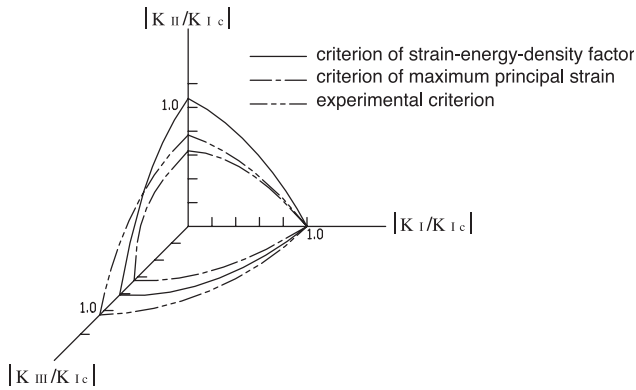


Fig. 3. Critical fracture curved surface of I–II–III model.

ness $K_{IC} = 0.93 \text{ KN/cm}^{3/2}$. The 3-D critical fracture curved surface was created in Fig. 3 using K_I/K_{IC} , $|K_{II}/K_{IC}|$ and $|K_{III}/K_{IC}|$ as the coordinate axes. The theoretical predictions of critical fracture curved surface from the strain–energy–density factor [6] and maximum principal strain theory [5] are also shown in Fig. 3 for comparison. It indicates that some differences exist between the experimental critical fracture curved surface and theoretical ones.

4. Conclusions

Twenty-five groups of critical stress intensity factors, from which 3-D critical fracture surface (fracture criterion) was regressed, were obtained based on the nondimensional stress intensity factor and critical load P_{cr} .

The fracture criterion expression derived in this research could be applied to the 3-D mixed-mode fracture problems of concrete structures such as dams, etc.

References

- [1] R. Widmann, Fracture mechanics and its limits of application in the field of dam construction, *Eng. Fract. Mech.* 135 (1/2/3) (1990) 532–539.
- [2] H.N. Linsbauer, A.R. Ingraffea, H.P. Rossmannith, Simulation of cracking in large arch dam, Part I, *J. Struct. Eng.* 115 (7) (1989) 1599–1630.
- [3] M.Z. Meinhard, A mixed hybrid finite element for three dimensional elastic crack analysis, *Int. J. Fract.* 45 (1990) 65–79.
- [4] M.K. Kassir, G.C. Sih, *Mechanics of Fracture, Three Dimensional Crack Problems*, vol. 2, Noordhoff International, Leyden, Netherlands, 1975.
- [5] G.C. Sih, Strain–energy–density factor applied to mode crack problems, *Int. J. Fract.* 10 (1974) 305–321.
- [6] M. Wang, Mixed mode strain fracture criterion, *J. Solid Mech.* 4 (1982) 571–581 (in Chinese).